Communications

Ordered Self-Assembly and Electronic Behavior of C$_{60}$–Anthrylphenylacetylene Hybrid**

Seok Ho Kang, Hong Ma, Mun-Sik Kang, Kyoung-Soo Kim, Alex K.-Y. Jen,* M. Hadi Zareie, and Mehmet Sarikaya*

The fullerene (C$_{60}$) molecule has very unique and attractive electronic, optical, and mechanical properties owing to its chemical properties and uniform, spherical, and nanoscale physical structure.[1] Recent studies revealed that thin films made of C$_{60}$ exhibit a wide range of interesting characteristics such as charge transport, photoconductivity, superconductivity (upon doping with alkali metals), and biological activities.[2–3] The development of new C$_{60}$-based thin-film materials relies strongly on the development of novel synthetic and processing methodologies to modify C$_{60}$. Such methodologies include tailoring functional groups on C$_{60}$ derivatives and covalently attaching fullerenes to solid-state supports to obtain a desirable optical or electronic response. Among many techniques explored, self-assembling C$_{60}$-based molecules on flat solid substrates has been found to be a good way to make thin films that also allow investigation of their physical properties, because self-assembled monolayers (SAMs) formed by chemisorption yield well-defined structures on substrates.[4] In the literature, there are many reports on attempts to construct SAMs of C$_{60}$ to produce highly ordered and densely packed structures on substrates,[5–11] and there has been some success in this respect[12] especially the recently observed noncovalently bonded C$_{60}$ at very low temperatures (5 K).[13] In a previous work related to the development of stable and ordered assemblies of conjugated molecular structures, we reported the self-assembly of (4-mercaptophenyl)anthrylacetylene (MPAA) on the surface of Au(111). These molecules tend to form highly ordered 2D stacked arrays through an interplay of strong π–π intermolecular stacking and chemisorptive gold–thiol interactions.[14] We also discovered that the electronic behavior of MPAA depends on its local ordering and the close stacking of the molecules in SAM films. Thus, on basis of the previous study, it may be possible to combine the excellent physical and chemical properties of C$_{60}$ with the advantages offered by the

[*] Dr. S. H. Kang, Dr. H. Ma, Dr. M.-S. Kang, Dr. K.-S. Kim,
Prof. A. K.-Y. Jen, Dr. M. H. Zareie, Prof. M. Sarikaya
Department of Materials Science and Engineering
University of Washington
Seattle, WA 98195-2120 (USA)
Fax: (+1) 206-543-3100
E-mail: ajen@u.washington.edu
sarikaya@u.washington.edu

Supporting information for this article is available on the WWW under http://www.angewandte.org or from the author.

controlled nanoscale ordering of MPAA-based SAMs. The hybridization of these two functional molecules and their stable assemblies may introduce new electrical or optical properties. To achieve this, a new synthetic methodology had to be developed to covalently connect these two molecules as a stable entity. Herein we report the design, synthesis, self-assembly, and functional characteristics of the new hybrid molecule.

In our molecular design, we took advantage of the MPAA moiety to form a rigid and stable footing on gold substrates for constructing well-ordered C$_{60}$ films. Figure 1 shows the
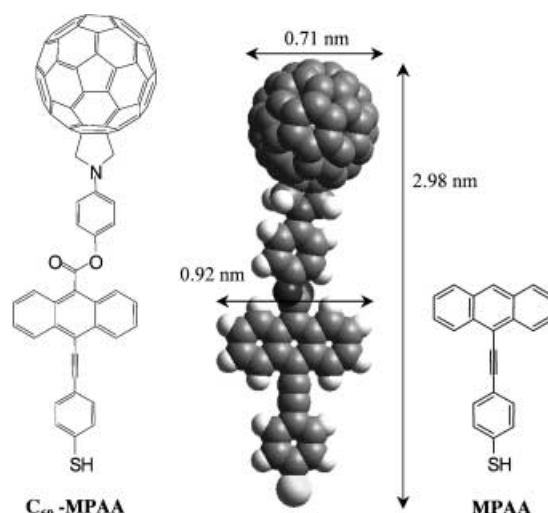

Figure 1. Schematic illustration of C$_{60}$–MPAA molecule based on MM2 calculation. The structure was optimized by force-field calculation by using Cerius 2 modeling program of Acelrys.

result of molecular modeling of C$_{60}$–MPAA (drawn by using the molecular mechanics 2, MM2, calculation method). The schematic suggests that the size of C$_{60}$ (0.71 nm) is slightly smaller than that of MPAA moiety (0.92 nm). The small difference (0.21 nm) between the size of the two molecules is a critical parameter that could favor the close-packing of C$_{60}$–MPAA into 2D arrays on a Au(111) substrate.

In our study, the C$_{60}$–MPAA hybrid molecule **4** was synthesized through the esterification of 9-(4-thioester-phenyl)-acetyleneanthracene-10-carboxylic acid **2** with *N*-(4-hydroxyphenyl)-3,4-fulleropyrrolidine **3** in the presence of a trace amount of trifluoroacetic anhydride as catalyst (Scheme 1). We employed the 1,3-dipolar cycloaddition methodology to functionalize C$_{60}$ with azomethine ylides.[15] Paraformaldehyde, *N*-(4-hydroxyphenyl)glycine, and C$_{60}$ were heated in refluxing toluene to afford *N*-(4-hydroxyphenyl)-3,4-fulleropyrrolidine **3** in 33% yield. 9-(4-Thioesterphenyl)-acetylene-anthracene-10-carboxylic acid **2** was synthesized by the acid-catalyzed deprotection of its *tert*-butyl ester precursor **1**, which was synthesized as shown in Scheme 2. The resulting coupled molecule **4** has an axis of twofold symmetry that runs through the length of the hybrid object. This symmetry has a profound effect on the control of the intermolecular forces that lead to the close packing of C$_{60}$ on gold. All compounds were purified by column chromatog-

Scheme 1. Synthesis of C$_{60}$–MPAA with acetyl protection.

Scheme 2. Synthesis of 9-(4-thioesterphenyl)acetyleneanthracene-10-ester **1**.

(CV), with the molecules or assembly dissolved or immersed in a solvent mixture (toluene/acetonitrile = 4:1) that contained 0.1 M of Bu$_4$NPF$_6$ as electrolyte and swept at a rate of 100 mV s^{-1} (Figure 2). Both the C$_{60}$–MPAA hybrid, and the assembly on Au showed two electrochemically accessible and stable reduction states of C$_{60}$. The CV profile for the hybrid exhibited two well-resolved reversible redox waves at $E_{1/2}$ = -0.56 and -0.95 V versus Ag/AgCl. These values are typical for monofunctionalized C$_{60}$.[15] The first and the second peaks are attributed to successive one-electron reductions/oxidations of the C$_{60}$ moiety. The CV results of C$_{60}$–MPAA/Au SAM also reveal well-defined redox waves and indicate that the hybrid molecules are strongly adsorbed on the gold surface. Although the first and second reduction potentials of the assembled films have shifted slightly to negative potentials ($E_{1/2}$ = -0.61 and -0.99 V, respectively) compared to those of the hybrid molecule in solution (Figure 2), these results resemble those of previously reported C$_{60}$ SAMs.[16]

Figure 3 shows a high-resolution scanning tunneling microscopy (STM) image of the C$_{60}$–MPAA SAM on Au(111)/mica recorded at room temperature. Each bright sphere indicates where a C$_{60}$ core locates directly on top of an MPAA molecule. The image reveals a well-ordered 2D nanostructure that extends throughout a given textured Au grain. As shown in the power spectrum (Figure 3b) of the STM image (Figure 3a), the organization of the hybrid molecules in the self-assembled structure exhibits a pseudohexagonal arrangement. The oblique lattice formed by the hybrid molecule is characterized by a unit cell with $a = 1.00 \pm$

Figure 2. Cyclic voltammograms of C$_{60}$–MPAA (dotted line) and C$_{60}$–MPAA/Au (solid line) in toluene/acetonitrile = 4:1 with 0.1 M Bu$_4$NPF$_6$ at a sweep rate of 100 mV s^{-1}.

raphy to give analytically pure materials, and their chemical structures were fully confirmed by ^{1}H, ^{13}C NMR spectroscopy and mass spectrometry.

SAM of C$_{60}$–MPAA hybrid was prepared by immersing Au(111)/mica substrate in a solution of **4** in THF/EtOH (1:10) at 25°C for 24 h in the presence of a solution of ammonium hydroxide, thus hydrolyzing the acetyl protecting group. The thin film sample was then rinsed with THF and EtOH, and dried with a stream of nitrogen. The electrochemical properties of the C$_{60}$–MPAA hybrid as well as the SAM on Au were evaluated. This was carried out by using cyclic voltammetry
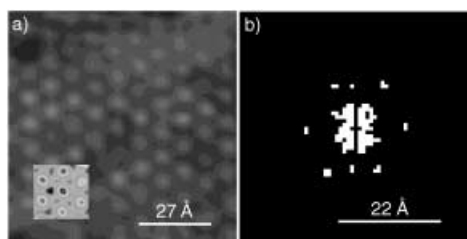
Figure 3. Room-temperature STM images of ordered assemblies of C$_{60}$–MPAA on Au(111) surface (constant current mode, U_t and average I are 200 mV and 100 pA, respectively). a) after 24 h self-assembly; inset: reconstructed image by using the transform in (b). b) Fourier transform of the periodic pattern shown in (a) reveals an oblique lattice.

0.25 nm, $b = 0.90 \pm 0.25$ nm; and the angle between them $\alpha = 62 \pm 0.5°$. It is well known that the self-assembly of C$_{60}$ molecules on Au(111) results in the formation of perfectly hexagonal lattices with lattice parameters of about 0.9 nm.[15,17–19] The observation that the C$_{60}$–MPAA hybrid does not form perfectly hexagonal lattices requires further consideration.

The C$_{60}$ molecule alone is spherical, and spherical particles on a flat surface organize into hexagonal lattice, the lowest energy state. In this supramolecular organization each particle has sixfold symmetry. However, as shown above, the hybrid molecule we synthesized forms an oblique structure with twofold symmetry (Figure 3b), probably because the C$_{60}$–MPAA hybrid molecule itself has twofold symmetry resulting from the asymmetric molecular architecture of the MPAA, that is, the planar MPAA part of the hybrid molecule is slightly larger than the C$_{60}$ part. While C$_{60}$ alone has a full 360° rotational freedom, this is not so true when it is tethered to the MPAA molecule and organized into a 2D ordered structure. Therefore, the twofold symmetry in the hybrid molecular architecture imposes a restriction on the rotation of the new molecule and forces it into an energetically more-favorable oblique-lattice conformation. This configuration is likely to correspond to a stable state at which centrally symmetric interactions among C$_{60}$ molecules and planar interactions among MPAAs are compromised. It has also been demonstrated, in our earlier study,[14] that the MPAA ordered structure has an oblique lattice with lattice parameters significantly different ($a = 0.76$ nm and $b = 1.15$ nm) than in the lattice formed by the hybrid molecule studied here.

In addition to the structures, the dimensions of the lattices formed by C$_{60}$ alone and that formed by hybridization with MPAA differ, providing clues to their relative stabilities. For example, a C$_{60}$ film deposited directly on Au(111) surface shows a close-packed but unstable structure composed of mobile hexagonal arrays with an intercluster spacing of 1.1 nm.[15,17–19] Many other self-assembled structures based on alkylthiol-terminated fullerenes, fullerene-phenanthrolines, and disulfide-terminated fullerenes have also been reported. However, none of these earlier structures seem to have the same level of stable ordering as the hybrid molecule studied here. This stability is possibly due to the fact that alkyl chains in these SAMs are more dynamic, resulting in a loosely

packed long-range organization of the molecular film.[5–11] Recently, it was reported that ordered C$_{60}$ nanostructures can form on top of SAMs of alkylthiol films (on a Au(111) substrate) at 5 K.[12–13] In this case, the C$_{60}$ molecules form closed packed hexagonal arrays with a nearest-neighbor distance of 1.0 nm. However, the resulting C$_{60}$ arrays are not stable at room temperature. This instability is probably due to the detachment of C$_{60}$ molecules from the alkylthiol along with their free rotation above the SAM film. In our work, the SAMs of the hybrid molecule, which is made up of C$_{60}$ covalently bonded to MPAA, exhibit a high degree of ordering even at room temperature. The stable and robust nanoscale self-assembly and the resulting structure is a result of the interplay of intermolecular interactions among π–π stacked MPAA molecules in addition to interactions among the C$_{60}$ molecules and the thiol–Au bonding.

We have also prepared composite samples of C$_{60}$–MPAA hybrid and MPAA molecules and observed their coassembly to assess their structure and corresponding electrical properties. Figure 4a is a room-temperature STM image that reveals
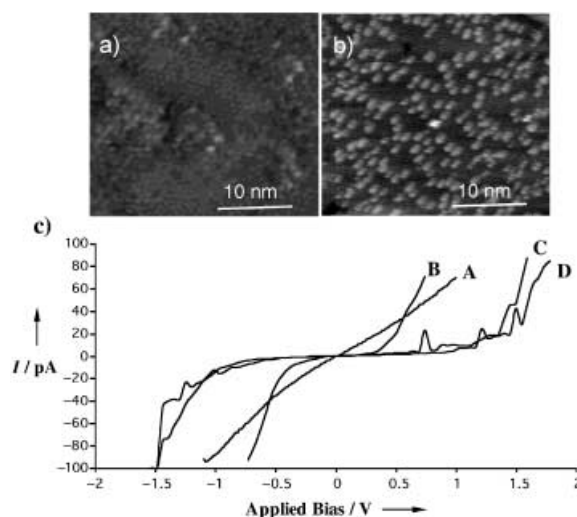

Figure 4. Room-temperature STM images of the molecular-ordered self-assemblies (both were recorded under constant current with U_t and average I being 200 mV and 100 pA, respectively). a) Assembly of C$_{60}$–MPAA observed after 24 h; b) Coassembly of C$_{60}$–MPAA and MPAA (ratio of compositions = 1:9) after 24 h. The bright spots in (b) corresponds to the aggregates of C$_{60}$–MPAA; c) Current-voltage characteristics of SAMs. A: Au(111); B: C$_{60}$ only; C: C$_{60}$-MPAA in the homoassembly; D: C$_{60}$-MPAA co-assembled into MPAA (1:9).

a long-range molecularly ordered homoassembly of C$_{60}$–MPAA on a gold substrate. On the other hand, Figure 4b reveals coassembled structure of the C$_{60}$–MPAA hybrid (10%) with MPAA (90%) molecules. In latter case, the C$_{60}$–MPAA molecules form small, stable island-like aggregates that are fairly homogeneously distributed within the matrix of ordered MPAA molecules. The bright spots in Figure 4b represent the constant-current STM images of the hybrid molecules that are taller than those of the matrix molecules (2.98 nm versus 1.2 nm). The C$_{60}$–MPAA islands in Figure 4b contain a small number of molecules (1 to 3) and

appear to be commensurate with the surrounding ordered molecular matrix, possibly a result of the twofold symmetry of the MPAA molecule in both regions.

We investigated electronic behavior of the C_{60}–MPAA SAMs by establishing their current/voltage (*I/V*) characteristics by scanning tunneling spectroscopy (STS; Figure 4c). The STS measurements were performed at a fixed tip–sample distance with the feedback loop being switched off. Each *I/V* curve was averaged over six successive voltage sweeps, with all six were typically within the measurement error. The time required for a complete spectroscopy measurement was below 1 second; therefore any influence of lateral drift was neglected.

Curves A, B, and C in Figure 4c show the *I/V* characteristics of bare Au(111), physically adsorbed C_{60} monolayer and homoassembled monolayer of C_{60}–MPAA on Au(111), respectively. Curve D in Figure 4c exhibits the *I/V* characteristics of the SAM of C_{60}–MPAA coassembled with MPAA. Both of the *I/V* curves of C_{60}–MPAA in homoassembly and coassembly show semiconducting behavior, evident when compared with the metallic characteristic of bare Au surface. The C_{60}–MPAA molecule, whether homoassembled or coassembled, has a much larger energy gap than that of pure C_{60} when it is directly physically adsorbed on Au. This difference is probably due to the fact that the introduction of anthryl-phenyl acetylene moiety changes the electronic characteristics of the C_{60}, which is verified by UV/Vis absorption spectra (reported elsewhere). Moreover, the STS spectra of the C_{60}–MPAA show multiple peaks in *I/V* curves (Figure 4c, curves C and D). These peaks resemble negative differential resistance (NDR) phenomenon reported earlier by Reed and co-workers.[20] The occurrence of the NDR effect is possibly due to the weak charge transfer between the MPAA and the electron-affinity of C_{60} at the molecular junction of C_{60}–MPAA. It should be noted that the *I/V* curves of the SAMs of neither C_{60} or MPAA[14] alone exhibit these peaks.

Another interesting point to note in the *I/V* curves corresponding to C_{60}–MPAA molecules in both homo and mixed states is that only weak (or no) apparent NDR-type peaks appear on the negative bias side. This finding may be an indication that charge transfer takes place more strongly in one direction, that is, from the electron-rich MPAA to the electron-deficient C_{60}. These peaks also exhibit very different bias voltage positions in the homo- and coassembled SAMs of C_{60}-MPAA (curves C and D in Figure 4c). The multiple peaks in *I/V* curves are especially clear in the coassembly state (Figure 4c, curve D) because of the measurements from isolated islands of C_{60}–MPAA. The differences in the characteristics of the peaks (number of peaks and their positions) may be due to a collective phenomena of different molecular surroundings of the C_{60}–MPAA molecules and their local ordering in these two SAMs; this would lead to different intermolecular interactions and changes in energy levels of molecular orbitals of the two assemblies. The more in-depth investigation of the electrical properties of these SAMs, especially verification of the possible NDR effect, could be carried out through STS measurements of the *I/V* characteristics by carefully isolating the hybrid molecules within the MPAA matrix, as planned in the near future.

In summary, we have designed and synthesized a novel functional hybrid molecule, C_{60}–MPAA, by taking advantage of the excellent physical and chemical properties of C_{60} and nanoscale ordering of anthryl-based SAMs. The self-assembled molecular films of C_{60}–MPAA exhibit stable and highly ordered 2D arrays that form an oblique lattice at room temperature. The self-assemblies of C_{60}–MPAA exhibit reversible electrochemical peaks and interesting electronic properties. The design strategy developed here should generally be applicable to other molecules for developing novel, well-ordered nanostructural assemblies and a wide range of thin film functional materials.

[1] a) C. A. Mirkin, W. B. Caldwell, *Tetrahedron* **1996**, *52*, 5113–5130; b) M. Prato, *Top. Curr. Chem.* **1999**, *199*, 173–187; c) G. Yu, J. Gao, J. C. Hummelen, F. Wudl, A. J. Heeger, *Science* **1995**, *270*, 1789.

[2] M. Prato, *J. Mater. Chem.* **1997**, *7*, 10970–11109.

[3] F. Diederich, M. Gómez-López, *Chem. Soc. Rev.* **1999**, *28*, 263–277.

[4] a) *Self-assembled Monolayers of Thiols* (Eds.: A. Ulman), Academic, San Diego, **1998**; b) A. Ulman, *Chem. Rev.* **1996**, *96*, 1533; c) A. R. Bishop, R. G. Nuzzo, *Curr. Opin. Colloid Interface Sci.* **1996**, *1*, 127; d) F. Schreiber, *Prog. Surf. Sci.* **2000**, *65*, 151; e) M. Mrksich, G. M. Whitesides, *Annu. Rev. Biophys. Biomol. Struct.* **1996**, *25*, 55.

[5] W. B. Caldwell, K. Chen, C. A. Mirkin, S. J. Babinec, *Langmuir* **1993**, *9*, 1945–1947.

[6] V. V. Tsukruk, L. M. Lander, W. J. Brittain, *Langmuir* **1994**, *10*, 996–999.

[7] X. Shi, W. B. Caldwell, K. Chen, C. A. Mirkin, *J. Am. Chem. Soc.* **1994**, *116*, 11598–11599.

[8] F. Arias, L. A. Godínez, S. R. Wilson, A. E. Kaifer, L. Echegoyen, *J. Am. Chem. Soc.* **1996**, *118*, 6086–6087.

[9] O. Domínguez, L. Echegoyen, F. Cunha, N. Tao, *Langmuir* **1998**, *14*, 821–824.

[10] Y.-S. Shon, K. F. Kelly, N. J. Halas, T. R. Lee, *Langmuir* **1999**, *15*, 5329–5332.

[11] S. Zhang, D. Dong, L. Gan, Z. Liu, C. Huang, *New J. Chem.* **2001**, *25*, 606–610.

[12] a) T. Sakurai, X. D. Wang, K. Q. Xue, Y. Hasegawa, T. Hashizume, H. Shinohara, *Prog. Surf. Sci.* **1996**, *51*, 263; b) R. J. Wilson, G. Meijer, D. S. Bethune, R. D. Johnson, D. D. Chambliss, M. S. de Vries, H. E. Hunziker, H. R. Wendt, *Nature* **1990**, *348*, 621; c) A. Marchenko, J. Cousty, *Surf. Sci.* **2002**, *513*, 233.

[13] a) J. G. Hou, J. L. Yang, H. Q. Wang, Q. X. Li, C. G. Zeng, L. F. Yuan, B. Wang, D. M. Chen, Q. S. Zhu, *Nature* **2001**, *409*, 304–305; b) L. F. Yuan, J. L. Yang, H. Q. Wang, C. G. Zeng, Q. X. Li, B. Wang, J. G. Hou, Q. S. Zhu, D. M. Chen, *J. Am. Chem. Soc.* **2003**, *125*, 169–172.

[14] M. H. Zareie, H. Ma, B. W. Reed, A. K.-Y. Jen, M. Sarikaya, *Nano Lett.* **2003**, *3*, 139–142.

[15] L. Echegoyen, L. E. Echegoyen, *Acc. Chem. Res.* **1998**, *31*, 593–601.

[16] H. Imahori, T. Azuma, A. Ajavakom, H. Norieda, H. Yamada, Y. Sakata, *J. Phys. Chem. B* **1999**, *103*, 7233–7237.

[17] R. J. Willson, G. Meijer, D. S. Bethune, R. D. Johnson, D. D. Chambliss, M. S. de Vries, H. E. Hunziker, H. R. Wendt, *Nature* **1990**, *348*, 621–622.

Communications

[18] L. D. Lamb, D. R. Huffman, R. K. Workman, S. Howells, T. Chen, D. Sarid, R. F. Ziolo, *Science* **1992**, *255*, 1413–1416.

[19] E. I. Altman, R. J. Colton, *Phys. Rev. B* **1993**, *48*, 18244–18249.

[20] a) J. Chen, M. A. Reed, A. M. Rawlett, J. M. Tour, *Science* **1999**, *286*, 1550; b) Y. Selzer, A. Salomon, J. Ghabboun, D. Cahen, *Angew. Chem.* **2002**, *114*, 855; *Angew. Chem. Int. Ed.* **2002**, *41*, 827; c) C. B. Gorman, R. L. Carroll, R. R. Fuierer, *Langmuir* **2001**, *17*, 6923; d) J. Cornil, Y. Karzazi, J. L. Brédas, *J. Am. Chem. Soc.* **2002**, *124*, 3516.